

PACS numbers: 42.65.Dr; 42.65.Es; 42.65.Hw
DOI: 10.1070/QE2007v037n01ABEH013265

Amplification of Stokes signals with phase conjugation by combined laser and SBS amplifiers

I.M. Bel'dyugin, V.F. Efimkov, I.G. Zubarev, S.I. Mikhailov, V.B. Sobolev

Abstract. **Various schemes for amplification of Stokes signals are investigated. Some new systems, such as an SBS amplifier in the transient amplification regime and a combined laser amplifier – SBS amplifier, are proposed and realised. Conditions are found under which amplification is accompanied by small distortions of the spatial structure of a signal. A two-pass system for small-signal amplification with phase conjugation is developed by using a PC mirror in the combined amplification system. The gains up to 10^{16} were obtained for the phase conjugation quality $\sim$80 %, the output energy $\sim$1 J, and pulse duration $\sim$30 ns.**

Keywords: *SBS amplifier, neodymium amplifier, SBS mirror, multipass systems.*

1. Introduction

The study of the ultimate parameters of amplifiers gives information on the fields and outlook for their applications. In this respect, SBS amplifiers seem quite attractive. They have large gains in very narrow amplification bands (see [1] and references therein). A disadvantage of these amplifiers is a high equivalent input noise. Thus, while the equivalent input power noise in usual laser amplifiers of pulsed signals upon detection of the amplified radiation within one spatial mode is equal to one photon in the amplification band ($P_{\rm noise} = h\nu\Delta\nu$), the number $k_{\rm B}T/(h\Omega)$ of noise photons for SBS amplifiers within the amplification band is $\sim 10^3 - 10^4$, where $k_{\rm B}$ is the Boltzmann constant, T is the absolute temperature of the medium, and Ω is the frequency of acoustic photons involved in the SBS process. Nevertheless, the absolute value of the equivalent input noise of SBS amplifiers is lower than that for most solid-state laser systems because the amplification bands differ by more than four – six orders in favour of SBS amplifiers.

In this connection it is quite reasonable to attempt to combine the advantages of SBS and solid-state laser amplifiers within one system. For this purpose, it is necessary to place in front of an SBS amplifier a solid-state laser amplifier with the gain exceeding the number of the equivalent input noise photons in the SBS amplifier. In this case, the combined amplifier can be almost identical to the laser amplifier with respect to the equivalent input noise, i.e. it will have in fact only one noise photon in the amplification band. However, the amplification band will be determined in this case by the band of the SBS amplifier, while the gain of the entire system will be equal to the product of the gains of combined amplifiers. Such investigations were performed by several research groups [2, 3]. However, in our opinion, the ultimate parameters of the systems used in these studies have not been realised and some specific features of such combined systems (amplifiers) have been neglected. These are first of all the possible distortions of amplified radiation in solid-state laser amplifiers and simultaneous consideration of transient and saturation effects for a specific shape of amplified pulses in SBS amplifiers.

I.M. Bel'dyugin 'Astrofizika' Research and Production Association, Volokolamskoe sh. 95, 125424 Moscow, Russia;
V.F. Efimkov, I.G. Zubarev, S.I. Mikhailov, V.B. Sobolev P.N. Lebedev Physics Institute, Russian Academy of Sciences, Leninsky prosp. 53, 119991 Moscow, Russia; e-mail: efimkov@sci.lebedev.ru

Received 29 May 2006; revision received 29 September 2006
Kvantovaya Elektronika **37** (1) 43 – 48 (2007)
Translated by M.N. Sapozhnikov

2. Experimental setup

Figure 1 shows the scheme of channels for formation of pump radiation for a SBS amplifier and the input Stokes signal. Master oscillator (*1*) was a passively Q-switched neodymium glass laser with selection of the longitudinal and transverse modes, which emitted 50-ns, 20-mJ pulses in the single-frequency and single-mode regime.

The laser radiation passed through Faraday isolator (*2*), aperture (*3*) of diameter 4 mm, and preamplifier (*4*) and was split in beamsplitter (*5*) into two beams directed by polarisers (*7*) to the corresponding channels. One of the beams is directed to a Stokes signal generator [a lens with the focal distance $f = 30$ cm and a cell with a mixture of Xe ($p = 39$ atm) and SF_6 ($p = 10$ atm) at a total pressure of 49 atm]. Radiation reflected from the cell at the Stokes frequency passes through a polariser, Faraday isolator (*2*), and optical attenuator of the Stokes signal (*11*). Two Faraday isolators (*2*) protect the Stokes signal generator and master oscillator from the amplified backward Stokes radiation (see below). The energies and angular characteristics of the input ($E^{\rm in}$, $\theta^{\rm in}$) and amplified backward ($E^{\rm out}$, $\theta^{\rm out}$) Stokes signals are measured by systems (*13*) and (*14*). The second beam from the master oscillator is reflected from highly reflecting mirror (*6*) and also passes through a polariser. Soft aperture (*10*) of diameter 6 mm selects the central part of this beam with almost uniform cross-sectional intensity distribution. Two Fresnel rhombs (*8*) rotate by 90° the polarisation plane of radiation that twice

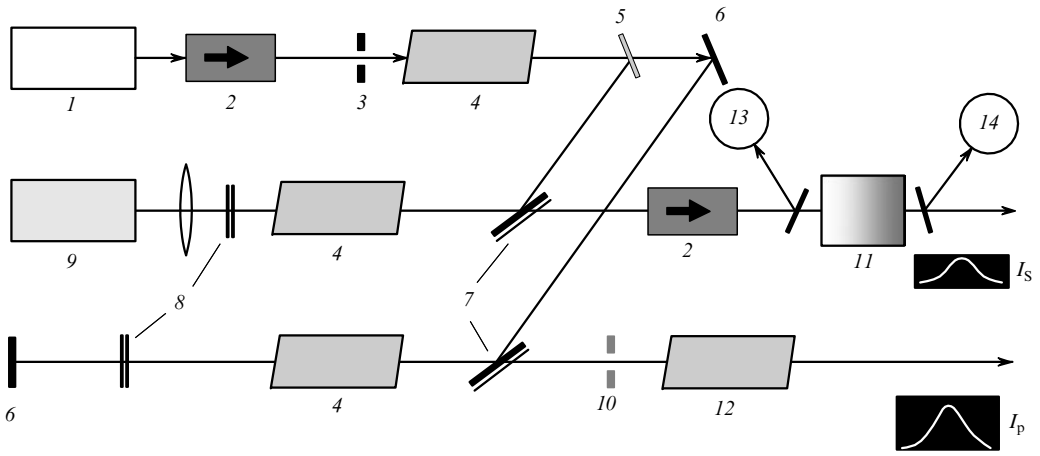

Figure 1. Scheme of formation of the pump radiation and Stokes signal: (*1*) master oscillator; (*2*) Faraday isolator; (*3*) aperture; (*4*) preamplifier; (*5*) beamsplitter; (*6*) highly reflecting mirror; (*7*) polarisers; (*8*) Fresnel rhomb; (*9*) Stokes signal generator; (*10*) soft aperture; (*11*) calibrated optical attenuator; (*12*) final pump radiation amplifier; (*13*, *14*) systems for recording parameters of the input and output pulses; I_S and I_p are the Stokes and pump signal intensities, respectively.

passed through them. In this way, the Stokes signal and pump radiation of the SBS amplifier is formed.

An important element of this scheme is optical attenuator (*11*) with the attenuation factor K_{att}. It should provide the controllable variation in the input Stokes pulse energy in a broad range exceeding twelve orders of magnitude. The pulse energy was measured with integrating photodiodes whose output signals were fed to two-channel digital oscilloscopes. Photodiodes have no such broad dynamic range. Crossed polarisers, in particular, Glan–Thomson prisms, which are often used to attenuate optical signals, also cannot provide such a broad dynamic range. This range can be formally covered by using a set of neutral filters. However, it should be taken into account that we use almost monochromatic radiation in our experiments. Therefore, the possible interference of radiation reflected from filter surfaces, both inside them and in the gap between them, can cause very large and uncontrollable variations in total transmission. Because of this, we used an attenuator that differs from the attenuator developed by us earlier [1] in that it contains four sections rather than three (Fig. 2).

The input Stokes radiation incident on plane–parallel glass plates is polarised in the incidence plane (p polarisation). The angle of incidence ($\sim$23.5°) was chosen so that for the refractive index $n = 1.506$ the attenuation factor for radiation reflected twice from the surface of each of the plates was 10^3. The diameter of the input beam was $\sim$3 mm and the distance between the centres of the beams emerging from the plates was $\sim$23 mm. By varying the configuration of apertures and using a compensating plate [1], we could obtain the attenuation factor K_{att} equal to 10^{3m}, were $m = 1$, 2, 3, 4. In particular, Fig. 2 corresponds to $K_{att}^{(m=4)} = 10^{12}$ if any of the apertures [(*4*) or (*8*)] is removed, we obtain $K_{att}^{(m=2)} = 10^6$; if both diagrams are removed, we obtain $K_{att} = 1$. In this case, radiation emerging from the attenuator always propagates along the same path. Small Fresnel radiation losses on surfaces of the plates are automatically taken into account by the method of relative gain measurements (see below). The attenuation factor could be also more continuously varied by using two neutral filters with attenuation factors 7 and 25 which were placed on both sides of attenuator (*11*). Due to their high optical quality, these filters did not violate the adjustment of the system.

Figure 3 presents the scheme of a combined amplifier. Lens (*9*) with $f = 3.5$ m produces the image of soft aperture [(*10*) in Fig. 1] at the centre of SBS amplifier (*6*). The pump beam has almost constant diameter $\sim$4 mm and quite uniform transverse intensity distribution over the entire length of the SBS amplifier. The input Stokes beam of diameter $\sim$2.5 mm is amplified in three-pass neodymium glass amplifier (*1*) and intersects the pump beam at a small angle, being always inside the pump beam within the SBS amplifier. This provides the maximum SBS gain and allows the use of the plane wave approximation. The SBS amplifier is a 50-cm cell with optical diameter 20 mm. The cell is filled with the same mixture as the Stokes signal generator. To

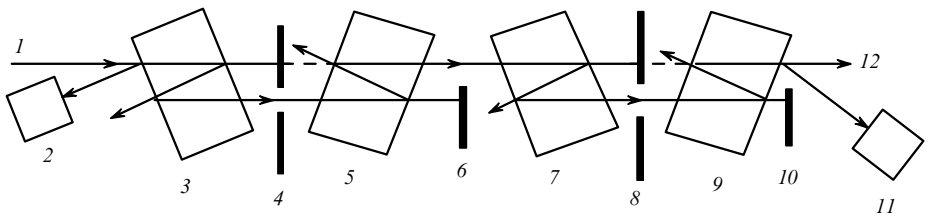

Figure 2. Optical scheme of the Stokes signal attenuator [(*11*) in Fig. 1]: (*1*) input Stokes signal; (*2*) photodetector measuring the input signal; (*3*, *5*, *7*, *9*) plane–parallel glass plates (∅ 60 × 40 mm); (*4*, *8*) apertures separating one of the beams propagated through the plate; (*6*, *10*) screens; (*11*) photodetector recording the radiation propagating in the direction opposite to the output attenuated signal (*12*); the dashed straight lines, which are absent in the real scheme, supplement the laser beam axis in the absence of apertures (*4*) and (*8*); refraction of the beams in plates is not shown.

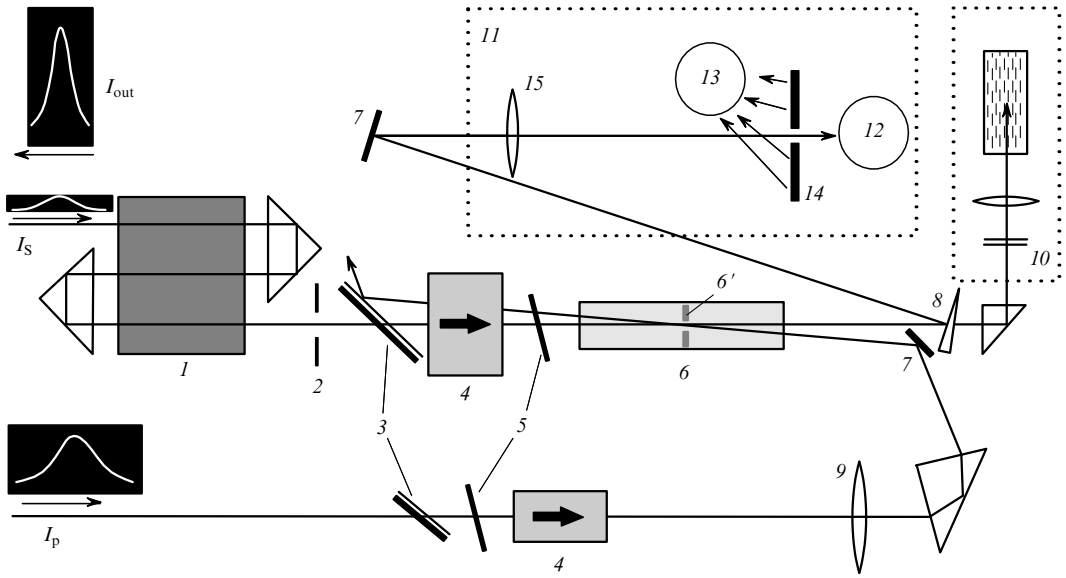

Figure 3. Optical scheme of the experiment: (*1*) three-pass neodymium glass amplifier; (*2*) filtering aperture; (*3*) polarisers; (*4*) Faraday isolator; (*5*) crystal quartz plates; (*6*) SBS amplifier; (*6′*) soft aperture image [(*10*) in Fig. 1]; (*7*) highly reflecting mirror; (*8*) optical wedge; (*9*) lens translating the soft aperture image [(*10*) in Fig. 1] to the centre of the SBS amplifier; (*10*) PC mirror rotating polarisation by 90°; (*11*) system for recording the energy of the amplified signal and noise; (*12*, *13*) photodiodes; (*14*) aperture; (*15*) lens; I_{out} is the output radiation intensity.

equalise the pressures and partial concentrations of mixtures, the cells were connected with a pipe and were kept in this state for a week. To achieve the maximum gain, the absence of depolarisation on the SBS amplifier cell windows is very important. Faraday rotators (*4*), quartz plates (*5*), and polarisers (*3*) are used to match polarisations of the interacting waves in the SBS amplifier and decouple the preliminary stages of the setup from backward radiation.

System (*11*) in Fig. 3 detects Stokes radiation amplified in the forward direction. This radiation is focused by lens (*15*) to aperture (*14*) (the angular size is $\sim 10^{-3}$ rad), and the pulse energy is measured with photodiode (*12*). The noise radiation of the SBS amplifier in the direction of the amplified Stokes signal is scattered from the mat surface of aperture (*14*) and is controlled with photodiode (*13*).

The main part of amplified radiation passes through glass wedge (*8*) and is incident on PC mirror (*10*) constructed by using the standard scheme with the rotation of polarisation of output radiation by 90° (CS_2 was used as an active medium). For a 30-ns pulse incident on PC mirror (*10*), the energy reflection threshold was ~ 0.5 mJ. The reflected PC radiation passes through the SBS amplifier in the backward direction (without amplification) and is amplified in three-pass amplifier (*1*), and its parameters are measured with system (*14*) (Fig. 1).

We showed earlier [1] that the maximum gain is realised in the transient SBS amplification regime if the Stokes pulse arrives to the amplifier by leaving behind the pump pulse by the time of the order of the lifetime of acoustic phonons of the active medium. The geometry of our setup could not provide such a delay of the pump pulse. In our case, this delay was $\Delta = 10$ ns, while the lifetime of optical phonons was $\tau_{ph} \approx 30$ ns.

3. Experimental results

The ultimate gain values were determined by the method of relative measurements. Signals were detected with integrating photodiodes whose output signals were fed to C8-9 digital oscilloscopes. Together with a neutral filter attenuating radiation by a factor of 25, each photodiode provided the linear dynamic range of signal measurements equal to 2.5×10^4. During measurements of the gains in the forward direction, PC mirror (*10*) (Fig. 3) was shielded by a screen.

First the gain K_{amp}^{Nd} of the three-pass neodymium glass amplifier was measured. For this purpose, apertures (*4*) and (*8*) were removed from the attenuator and its attenuation factor was assumed equal to unity. Then, the pump pulse of the SBS amplifier was shut down and pump flashlamps of the three-pass neodymium amplifier were switched off. In this state, a series of measurements of the parameters of the Stokes pulse propagating in the passive amplification path was performed. Based on these measurements, the quantity (for passive conditions)

$$\bar{T}_{pas} = \overline{E_{pas}^{(12)}/E_{pas}^{in}} \tag{1}$$

was determined, where $E_{pas}^{(12)}$ is the signal detected with photodiode (*12*) in Fig. 3 and E_{pas}^{in} is the signal detected with photodiode (*13*) in Fig. 1. Then, aperture (*4*) or (*8*) was introduced into the attenuator (Fig. 2). The attenuation factor was $K_{att}^{(2)} = 10^6$. The output signals $E^{(12)}$ and E^{in} of these photodiodes were detected again, but now the pump flashlamps of the three-pass neodymium glass amplifier were switched on. Then, the average value of the gain was calculated:

$$\bar{K}_{amp}^{Nd} = K_{att}^{(2)} \frac{\overline{E^{(12)}/E^{in}}}{\bar{T}_{pas}}. \tag{2}$$

For the maximum supply voltage of flashlamps, this value was $\bar{K}_{amp}^{Nd} \simeq (8 \pm 1) \times 10^3$. Due to a special arrangement of three passages of the Stokes signal in the active rod (without intersection of the beams), the amplifier was stable even for such a large gain and was far from self-excitation.

As a result, the amplifier noise was small, did not exceed the sensitivity threshold of photodiode (*12*) (Fig. 3) and had no effect on the measurements.

Our measurements showed that, if the pump pulse energy E_p did not exceed $\sim$300 mJ, the intrinsic noise of the SBS amplifier did not exceed 1 % of this value. Further measurements were performed for this pump energy. First a series of measurements of the intrinsic noise of the SBS amplifier was performed in the absence of the input Stokes signal and, as a result, the quantity

$$\bar{T}_n = \overline{E_n^{(12)}/E_n^{(13)}} \tag{3}$$

was determined, where $E_n^{(12)}$ and $E_n^{(13)}$ are signals detected with photodiodes (*12*) and (*13*) in Fig. 3. Then, the gain K_{amp}^{SBS} of the SBS amplifier was measured for different attenuation factors K_{att} of the optical attenuator (Fig. 1) when the pump flashlamps of the three-pass laser amplifier were switched off. Taking into account (1) and (3), it was obtained that

$$K_{amp}^{SBS} = K_{att}\overline{\left[\frac{E^{(12)} - \bar{T}_n E^{(13)}}{E^{in}}\right]}\bar{T}_{pas}^{-1}. \tag{4}$$

The corresponding dependence is presented in Fig. 4. The maximal achieved gain was $K_{amp}^{SBS} \simeq (2 \pm 1) \times 10^9$. In this case, the energy E_{amp}^{S} of the amplified Stokes signal at the output of the SBS amplifier was $\sim(3 \pm 1) \times 10^{-3}$ J. Figure 4 also presents the results of numerical simulation of the gain, which was performed taking into account the gain saturation and the transient nature of SBS in the plane wave approximation for lifetimes of acoustic phonons $\tau_{ph} = 20$, 30, and 40 ns and the maximum stationary gain increment $\Gamma = gI_{max}L = 75$ (where g is the gain, I_{max} is the maximum pump intensity, and L is the active medium length). Note that calculations were performed taking into account the real temporal behaviour of the interacting pulses. One can see that for $\tau_{ph} = 30$ ns, the experimental data almost completely agree with calculations. This value of τ_{ph} is also in good agreement with data reported in [4].

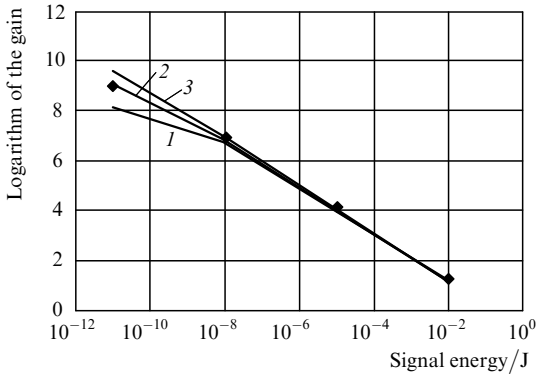

Figure 4. Dependences of the SBS amplifier gain on the input signal energy. Squares are experiment, solid curves are the results of the numerical simulation of the gain for the fixed maximum pump intensity and lifetimes of acoustic phonons $\tau_{ph} = 40$ (*1*), 30 (*2*), and 20 ns (*3*).

For the gain values $\sim 10^9$ obtained in our experiments, the saturation of the SBS amplifier becomes noticeable. However, it is practically impossible to reduce the input signal to obtain a higher amplification. The matter is that the SBS amplifier noise is coherent and interferes with the field of the amplified Stokes signal, although the phases of the noise waves change statistically from pulse to pulse. Therefore, if the fields of the noise radiation and amplified signal are comparable, their interference leads to strong radiation intensity fluctuations in the direction of the amplified signal from pulse to pulse because the phases of the amplified noise field are arbitrary. And if we wish not simply to detect a signal by multiple accumulations of measurements but to use each of the amplified pulses, the field of the amplified Stokes signal should exceed by several times the noise field of the SBS amplifier (Fig. 5).

Figure 5 presents the photographs of the radiation distribution emerging from the SBS amplifier, obtained on a photosensitive plate placed in front of PC mirror (*10*) (Fig. 3) for different amplitudes of input Stokes signals. After attenuation of the input signal by a factor of 10^{13}, the output signal was distinctly observed against the noise background only in one from the three cases (Fig. 5c). This quite 'unfavourable' effect, which can be called destructive interference, prevents the separation of the small input signal against the amplified noise background in each particular realisation. When the input signal was increased by an order of magnitude, the output signal could be reliably detected in each flash not only due to the increase in its intensity but also due to a partial suppression of the noise generation by the signal [5].

Then, we measured similarly the gain of the entire system in the forward direction upon the combined action of the SBS and laser amplifiers. The maximum gain $K_{amp}^{(+)}$ was $\sim(2 \pm 1) \times 10^{12}$, which is somewhat lower than the product of the gains of amplifiers measured separately. We explain this by the deformation of the wave front and the Stokes signal shape during amplification in the three-pass laser amplifier, both static and dynamical. The matter is that, according to our estimates, the width of the SBS amplification band for the gas mixture that we used is $\sim 3 \times 10^{-4}$ cm^{-1}. Therefore, the slightest perturbations of

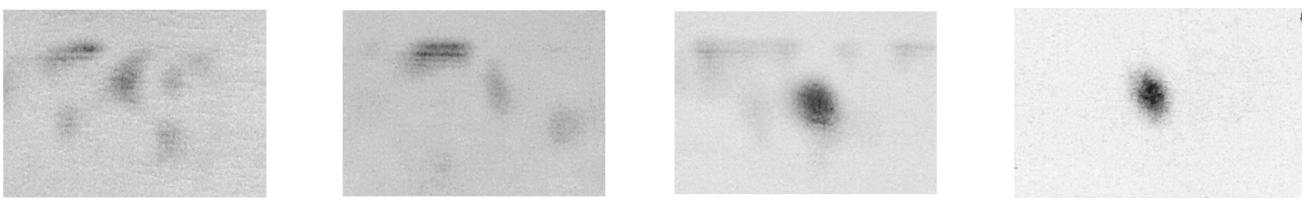

Figure 5. Photographs of the amplified radiation on the input aperture of the PC mirror: the input signal is attenuated by a factor of 10^{13} (a – c); the input signal is attenuated by a factor of 10^{12}, and a ten-fold attenuator is placed in front of the photographic plate (d).

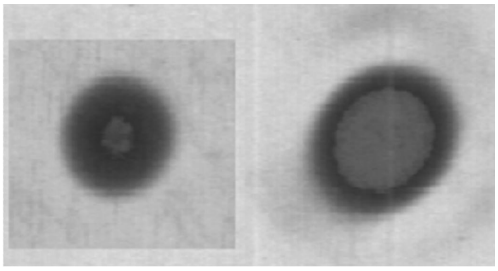

a b

Figure 6. Photographs of the signal field distribution after signal propagation through the three-pass neodymium glass amplifier in the unpumped (a) and pumped (b) states.

the spectrum of the input (in the SBS amplifier) Stokes signal reduce the gain. This is confirmed indirectly by the distortion of the spatial structure of the Stokes beam after three-pass amplification in the neodymium glass. The corresponding photographs of the transverse structure of the beam at the amplifier output in the passive and excited states are shown in Fig. 6.

For the maximum gain of the combined amplifier in the forward direction, the energy of the amplified Stokes signal exceeds the threshold energy of the PC mirror by several times (Fig. 3). In this case, the reflection coefficient was 50 % – 60 %. For this reason, the Stokes signal amplified in the forward direction is reflected from the PC mirror, propagates in the backward direction through the amplification path, and is amplified again in the three-pass neodymium glass amplifier. When passive amplifiers are used, the non-attenuated Stokes signal is also reflected from the PC mirror and its energy E^{out} is detected with a photodiode of measurement system (*14*) (Fig. 1). By performing, as usual, a series of measurements, we calculate the quantity (for passive conditions)

$$\bar{T} = \overline{E^{\text{out}}_{\text{pas}}/E^{\text{in}}_{\text{pas}}}. \qquad (5)$$

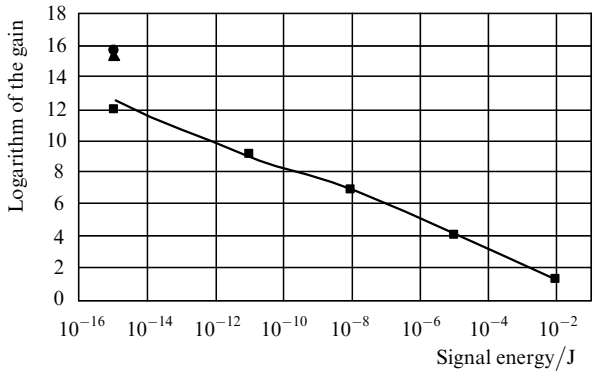

Figure 7. Dependence of the gain of the neodymium amplifier – SBS amplifier system on the input signal energy. The first four squares ■ to the right correspond to the gain obtained when the neodymium amplifier was switched off; the fifth square – to the gain obtained when the neodymium amplifier was switched on. The triangle ▲ corresponds to the gain in the two-pass amplifier with PC mirror (*10*) (Fig. 3); the circle ● corresponds to the gain of the three-pass neodymium amplifier calculated taking into account the gain saturation in the neodymium rod, losses, and the spatial distribution of the amplified pulse energy in the geometrical optics approximation.

Then, we set the attenuation factor of the attenuator equal to $K_{\text{att}} = 6.25 \times 10^{13}$ to obtain the maximum gain of the combined amplifier in the forward direction. After a series of measurements, we calculate the gain of the system in the backward direction:

$$K^{(-)}_{\text{amp}} = K_{\text{att}} \frac{\overline{(E^{\text{out}}/E^{\text{in}})}}{\bar{T}}.$$

As a result, we obtain $K^{(-)}_{\text{amp}} \simeq (0.5 - 1) \times 10^{16}$.

In this case, the energy of the signal emerging in the backward direction was ~1 J. Figure 7 presents the dependence of the gain on the energy of the input Stokes signal for the entire range of measurements. In the two-pass amplifier, we also measured the angular energy distribution in the input signal and signal emerging in the backward direction by the self-calibration method based on recording the focal distributions of the energy of a successively attenuated beam. In particular, a mirror wedge with the known reflectance of working surfaces was used. The photographs of the corresponding distributions and the results of their processing are presented in Fig. 8. Photographs were obtained for the gain $K^{(-)}_{\text{amp}} \simeq 5 \times 10^{15}$. One can see that 97 % of the input radiation energy is concentrated within an angle of 10^{-6} sr. Within this angle, 85 % of the amplified radiation is concentrated, while 15 % of the energy is

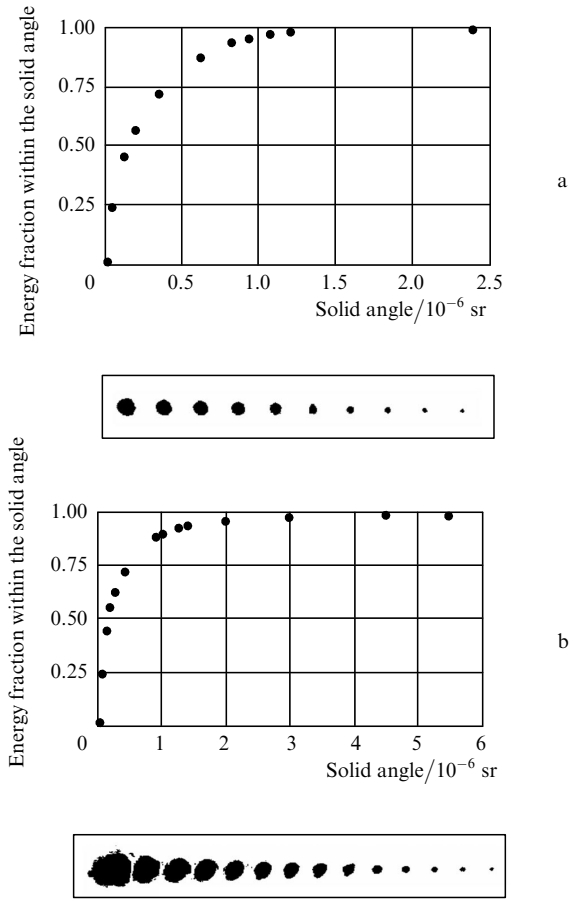

Figure 8. Dependences of the fractions of the input radiation energy (a) and amplified output signal (b) contained within the given solid angle on the value of this angle. Below: photographs of the distributions obtained by the self-calibration method.

distributed in rather broad but low-intensity tails. This means that the PC quality is no less than 0.8 in our case.

4. Conclusions

We have shown that SBS amplifiers operating in the transient scattering regime require higher pump intensities to obtain the same gain as in the stationary regime [6, 7]. However, such amplifiers also have a number of advantages. In particular, the duration of the amplified pulse in the transient regime decreases only by half (for active SBS media and pump pulse duration used in our experiments). This advantage is important for a combined amplifier if it is necessary to saturate a laser amplifier, for example, a neodymium glass amplifier by the amplified pulse. As for the maximum small-signal gains, they are determined by the self-excitation conditions of the amplifiers and are the same for stationary and transient scattering regimes.

References

1. Bel'dyugin I.M., Efimkov V.F., Zubarev I.G., Mikhailov S.I. *J. Russian Laser Research*, **23** (1), 1 (2005).
2. Bespalov V.I., Pasmanik G.A. *Nelineinaya optika i adaptivnye lazernye sistemy* (Nonlinear Optics and Adaptive Laser Systems) (Moscow: Nauka, 1986).
3. Gross R.W.F., Garman-DuVall L., Amimoto S.T. *Opt. Lett.*, **17**, 82 (1992).
4. Mak A.A., Soms L.I., Fromzel' V.A., Yashin V.E. *Lazery na neodimovom stekle* (Neodymium Glass Lasers) (Moscow: Nauka, 1990), p. 101.
5. Bel'dyugin I.M., Efimkov V.F., Zubarev I.G., Mikhailov S.I. Prepring FIAN, No. 18 (Moscow, 2003).
6. Bel'dyugin I.M., Davydov V.V., Demkin V.K., Efimkov V.F., Zubarev I.G., Mikhailov S.I., Sobolev V.B. *Kvantovaya Elektron.*, **31**, 709 (2001) [*Quantum Electron.*, **31**, 709 (2001)].
7. Scott A.M., Watkins D.E., Tapster P. *J. Opt. Soc. Am. B*, **7** (6), 929 (1990).